J|A|C|S
ARTICLES
Published on Web 08/19/2004

Modeling Branched Polyethylene: Copolymers Possessing Precisely Placed Ethyl Branches

John C. Sworen, Jason A. Smith,† Jessica M. Berg, and Kenneth B. Wagener*

Contribution from The George and Josephine Butler Polymer Research Laboratory, Department of Chemistry, University of Florida, Gainesville, Florida 32611-7200

Received April 14, 2004; E-mail: wagener@chem.ufl.edu

Abstract: A structural investigation of precise ethylene/1-butene (EB) copolymers has been completed using step polymerization chemistry. The synthetic methodology needed to generate four model copolymers is described; their primary and higher level structure is characterized. The copolymers possess an ethyl branch on every 9th, 15th, and 21st carbon along the backbone of linear polyethylene. Melting points and heats of fusion decrease with increased branch frequency. Differential scanning calorimetry and infrared spectroscopy show highly disordered crystal structures favoring ethyl branch inclusion. On the other hand, the EB copolymers contain high concentrations of kink and gauche defects independent of branch frequency. These model copolymers are compared with random copolymers produced using traditional chain chemistry and previously synthesized ADMET EP copolymers.

Introduction

Macromolecules based on ethylene and centralized around their copolymerization with α-olefins have been studied for more than 60 years. These branched copolymers have garnered much attention due to their enhanced mechanical properties, structural simplicity, and industrial importance. However, the inability to predict structure property functions for these simplest of polymers has led them to be among the most thoroughly studied macromolecules. Although such factors as mode of polymerization (radical, Ziegler−Natta, metallocene, etc.), catalyst choice, reaction temperature/pressure, and molar mass bare significant importance on ethylene/α-olefin copolymers, the short-chain branching (SCB) content and its distribution are the most prominent factors in linear low-density polyethylenes (LLDPEs).[1]

Linear low-density polyethylene is a statistical copolymer of ethylene and an α-olefin (butene, hexene, and octene) where the type, concentration, and distribution of these branches vary and are highly dependent on the chosen polymerization mechanism. Typically, these random copolymers are produced using Ziegler−Natta,[2,3] metallocene catalysts,[4−6] and anionically synthesized hydrogenated butadienes,[7,8] and when using other late transition metals.[9,10] Similar to the results obtained for ethylene/propylene (EP) copolymers,[11] studies on randomly branched ethylene/butylene (EB) copolymer systems have shown that the density, enthalpy, degree of crystallinity, and peak melting/crystallization points all decrease as the amount of defect content (ethyl branch) is increased. In the past, the interest of EB copolymers has been limited relative to ethylene/propene versions of LLDPE. These butylenes-based copolymers and homopolymers have garnered attention due to their unusual combination of toughness and flexibility as well as their

† Current address: Milliken & Co., Spartanburg, SC.

(1) (a) Shirayama, K.; Okada, T.; Kita, S. *J. Polym. Sci., Part 1: Gen. Pap.* **1965**, *3*, 907. (b) Shirayama, K.; Kita, S.; Watabe, H. *Makromol. Chem.* **1972**, *151*, 97. (c) Bergstrom, C.; Avela, E. *J. Appl. Polym. Sci.* **1979**, *23*, 163. (d) Wild, L.; Ryle, T. R.; Knobeloch, D. C.; Peat, I. R. *J. Polym. Sci., Polym. Phys. Ed.* **1982**, *20*, 441. (e) Schouterden, P.; Groenickx, G.; Van des Heijden, B.; Jansen, F. *Polymer* **1987**, *28*, 2099.
(2) (a) Forte, M.; Vieira da Cunha, F.; Zimnoch dos Santos, J.; Zacca, J. *Polymer* **2003**, *44*, 1377. (b) Usami, T.; Gotoh, Y.; Takayama, S. *Macromolecules* **1996**, *19*, 2722. (c) Union Carbide Jpn. Pat. JP 54-148093, 1979. (d) Showa Denko Jpn. Pat. JP 55-3459, 1980. (e) CdF Chimie Jpn. Pat. JP 55-131007, 1980. (f) Mitsui Petrochemical Jpn. Pat. JP 53-92887, 1978.
(3) Sumitomo Chemical Co. Jpn. Pat. JP 880-23561, 1980.
(4) (a) Villar, M. Z.; Ferreira, M. L. *J. Polym. Sci., Part A: Polym. Chem.* **2001**, *39*, 1136. (b) Kaminsky, W.; Hähnsen, H.; Külper, K.; Wöldt, R. U.S. Pat. 4542199, 1985. (c) Sherman, L. M. *Plast. Technol.* **1967**, *42*, 38. (c) Seppälä, J. V.; Koivumäki, J.; Liu, X. *J. Polym. Sci., Part A: Polym. Chem.* **1993**, *31*, 3347.
(5) Eynde, S. V.; Mathot, V.; Koch, M. H. J.; Reynaers, H. *Polymer* **2000**, *41*, 3437.
(6) (a) Mäder, D.; Heinemann, J.; Walter, P.; Mülhaupt, R. *Macromolecules* **2000**, *33*, 1254. (b) Minick, J.; Moet, A.; Hiltner, A.; Baer, E.; Chum, S. P. *J. Appl. Polym. Sci.* **1995**, *58*, 1371.
(7) (a) Fernyhough, C. M.; Young, R. N.; Poche, D.; Degroot, A. W.; Bosscher, F. *Macromolecules* **2001**, *34*, 7034. (b) Balsara, N. P.; Fetters, L. J.; Nadjichristidis, N.; Lohse, D. J.; Han, C. C.; Graessley, W. W.; Krishnamoorti, R. *Macromolecules* **1992**, *25*, 6137. (c) Doi, Y.; Yano. A.; Soga, K.; Burfield, D. R. *Macromolecules* **1986**, *19*, 2409.
(8) (a) Gerum, W.; Höhne, G. W. H.; Wilke, W.; Arnold, M.; Wegner, T. *Macromol. Chem. Phys.* **1995**, *196*, 3797. (b) Krigas, T. M.; Carella, J. M.; Struglinski, M. J.; Crist, B.; Graessley, W. W.; Schilling, F. C. *J. Polym. Sci., Polym. Phys. Ed.* **1985**, *23*, 509. (c) Rachapudy, H.; Smith, G. G.; Raju, V. R.; Graessley, W. W. *J. Polym. Sci., Polym. Phys. Ed.* **1979**, *17*, 1211.
(9) Bauers, F. M.; Chowdhry, M. M.; Mecking, S. *Macromolecules* **2003**, *36*, 6711.
(10) (a) Rangwala, H. A.; Dalla Lana, I. G.; Szymura, J. A.; Fiedorow, R. M. *J. Polym. Sci., Part A: Polym. Chem.* **1996**, *34*, 3379. (b) Xiao, S.; Lu, H. *J. Mol. Catal.* **1992**, *76*, 195. (c) Zakharov, V. A.; Yechevskaya, L. G.; Bukatov, G. D. *Makromol. Chem.* **1989**, *190*, 559.
(11) (a) Ungar, G.; Zeng, X. *Chem. Rev.* **2001**, *101*, 4157. (b) Bracco, S.; Comotti, A.; Simonutti, R.; Camurati, I.; Sozzani, P. *Macromolecules* **2002**, *35*, 1677. (c) Zhang, F.; Song, M.; Lü, T.; Liu, J.; He, T. *Polymer* **2002**, *43*, 1453. (d) DesLauriers, P. J.; Rohlfing, D. C.; Hsieh, E. T. *Polymer* **2002**, *43*, 159. (e) Starck, P.; Malmberg, A.; Löfgren, B. *J. Appl. Polym. Sci.* **2002**, *83*, 1140. (f) Pak, J.; Wunderlich, B. *Macromolecules* **2001**, *34*, 4492. (g) Haigh, J. A.; Nguyen, C.; Alamo, R. G.; Mandelkern, L. *J. Therm. Anal. Calorim.* **2000**, *59*, 435.

10.1021/ja047850p CCC: $27.50

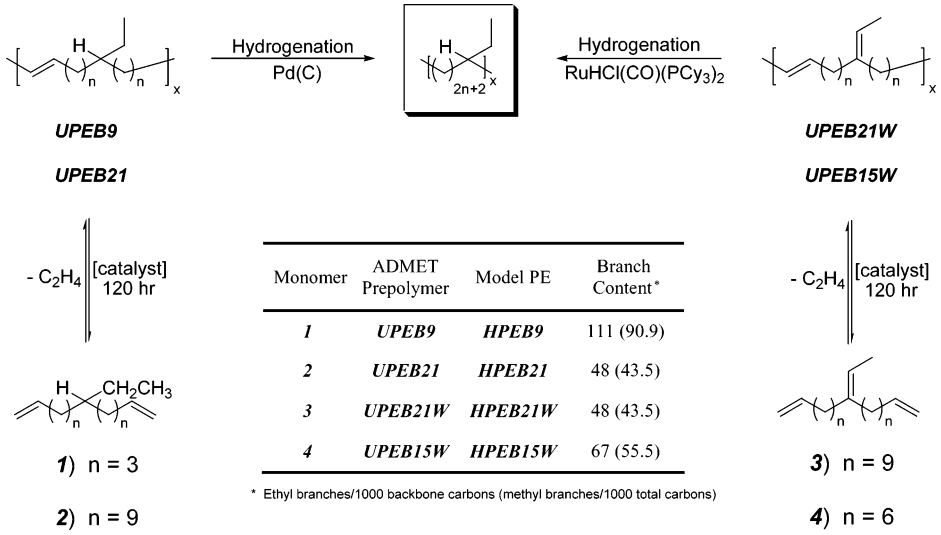

Monomer	ADMET Prepolymer	Model PE	Branch Content*
1	***UPEB9***	***HPEB9***	111 (90.9)
2	***UPEB21***	***HPEB21***	48 (43.5)
3	***UPEB21W***	***HPEB21W***	48 (43.5)
4	***UPEB15W***	***HPEB15W***	67 (55.5)

* Ethyl branches/1000 backbone carbons (methyl branches/1000 total carbons)

Figure 1. Controlling ethyl branch content using ADMET polymerization.

resistance to creep and external stress.[12] However, the synthetic methodology used to study these copolymers may produce unwanted side reactions and as a result unknown primary structures. These defects, even in small quantities, can alter the polymer's macromolecular behavior and thermal response depending on their frequency and identity.

Recently we presented a way to obviate the random nature of branching in polyethylene along with unwanted side products.[13,14] Doing so has been accomplished using the clean, step polymerization chemistry offered by acyclic diene metathesis (ADMET). This mild chemistry avoids chain transfer and other catalyst "mistakes" encountered during chain propagation processes, thereby producing a branched polymer with a homogeneous composition distribution and known branch identity (Figure 1).

A short time ago we reported the synthesis and thermal behavior for a series of five model EP copolymers in which the methyl branch was precisely placed on each 9th, 11th, 15th, 19th, and 21st carbon along the backbone, respectively.[14] We have also reported polyethylene-containing precise methyl content, but with a statistical placement along the backbone using ADMET copolymerization.[15] The thermal behavior and morphological analysis for this series of EP copolymers have yielded unique results, in effect creating a new class of PE-based materials using metathesis, based on the structural control offered by precise branch identity coupled with their precise or random placement.

In an effort to extend our LLDPE structural library, a synthetic methodology was sought to lengthen the alkyl branch in these model materials. This has proven to be a difficult task, for the structural simplicity of symmetrically disposed, substituted dienes is deceptive. We now report the successful synthesis of α,ω-diene monomers in which the ethyl branch has been symmetrically substituted on the hydrocarbon backbone. The ADMET polymerization of these monomers and subsequent hydrogenation has yielded the first ADMET model EB copolymers wherein the ethyl branch is placed on each 9th, 15th, and 21st carbon along the backbone (Figure 1). Herein, we present the monomer/polymer synthesis, characterization, and thermal analysis for these new LLDPE model materials.

Results and Discussion

(A) Monomer Synthesis and Characterization. The mild chemistry afforded by ADMET polymerization has proven a useful mechanism for the modeling of perfectly branched structures.[13,14] The cornerstone of this perfectly branched PE model study has been to produce a monomer (α,ω-diene) with pure α-olefin functionality along with perfect branch identity (Figure 1). Fulfilling both requirements has proven difficult when expanding the branch length beyond the methyl group,[14] leading to significant effort in formulating a synthetic pathway that would successfully extend the branch identity without sacrificing the integrity of the diene. Several methodologies were investigated throughout the synthesis work to generate perfectly branched LLDPE materials; multiple synthetic procedures were used to complete this study starting either from ethyl acetoacetate (Figure 2), diethyl malonate (Figure 3), or ketodienes (Figure 4). The first successful synthetic strategy to produce a pure α,ω-diene monomer with a symmetrically substituted ethyl branch is presented in Figure 2.

The conditions in step 1 (Figure 2) were modified from the work of Krapcho et al.[16] Ethyl acetoacetate is deprotonated with base and readily effects the S_N2 displacement of bromide upon addition of 5-bromo-1-pentene. Subsequently, in the same pot, the monosubstituted product is reacted with a second equivalent of base and alkenyl halide, affording the disubstituted β-keto ester (**6**). Compound **6** was decarboxylated using a dimethyl sulfoxide (DMSO)/water/salt mixture[16] to produce an α,ω-diene with a pendant methyl ketone that is symmetrically substituted along the monomer backbone (7). Reduction using lithium aluminum hydride (LAH) yields the secondary alcohol (**8**), which is further tosylated (**9**). The reducing agent $Li(Et)_3BH$,

(12) (a) Al-Hussein, M.; Strobl, G. *Macromolecules* **2002**, *35*, 8515. (b) Lindegren, C. R. *Polym. Eng. Sci.* **1970**, *10*, 163.
(13) O'Gara, J. E.; Wagener, K. B.; Hahn, S. F. *Makromol. Chem., Rapid Commun.* **1993**, *14*, 657.
(14) Smith, J. A.; Brzezinska, K. R.; Valenti, D. J.; Wagener, K. B. *Macromolecules* **2000**, *33*, 3781.
(15) Sworen, J. C.; Smith, J. A.; Wagener, K. B.; Baugh, L. S.; Rucker, S. P. *J. Am. Chem. Soc.* **2003**, *125*, 2228.
(16) (a) Krapcho, A. P.; Weimaster, J. F.; Eldridge, J. M.; Jahngen, G. E., Jr.; Lovey, A. J.; Stephens, W. P. *J. Org. Chem.* **1978**, *43*, 138. (b) Krapcho, A. P. *Synthesis* **1982**, 805. (c) Krapcho, A. P. *Synthesis* **1982**, 893. (d) Krapcho, A. P.; Gowrikumar, G. *J. Org. Chem.* **1987**, *52*, 1880.

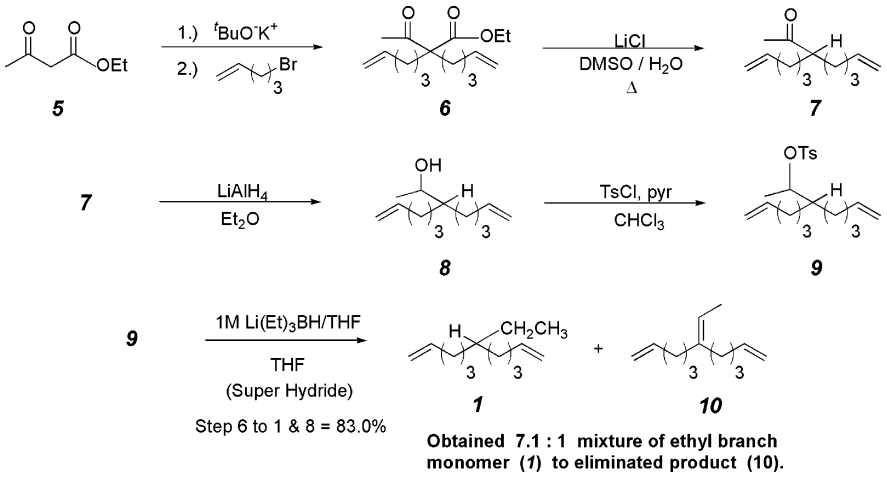

Figure 2. Ethyl-branch synthetic methodology for short methylene monomers.

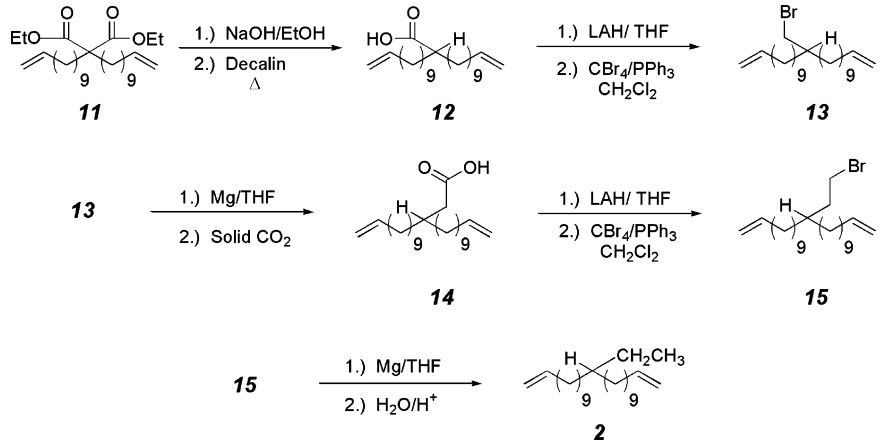

Figure 3. Synthesis for longer methylene run length monomers shown for 3-(10-undecenyl)-13-tetradecene (**2**).

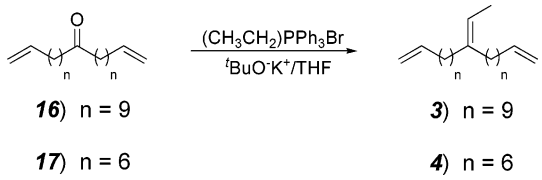

Figure 4. Synthesis of Wittig monomers.

coined Super Hydride, first employed by H. C. Brown and co-workers in the late 1970s, is used to reduce compound **9**.[17] This final step yields a mixture of the symmetrical diene of interest (**1**) and eliminated byproduct (**10**). These products can be separated using HPLC or careful column chromatography with hexane. The use of the hindered boron reducing agent is evident since the reduction of the tosylated alcohol (**9**) with LAH produces no traceable amount of compound **1**, whereas a 68% conversion was observed for the olefinic monomer **10**.

Although monomer **1** (three methylenes) was successfully produced by the method shown in Figure 2, difficulties were encountered when trying to synthesize monomers containing longer chain lengths. Complications arise during the reduction of the secondary tosylated or mesylated alcohol derivatives. The preferred synthesis for these longer run length monomers is shown in Figure 3, outlined for 3-(10-undecenyl)-13-tetradecene (**2**), to produce precisely placed ethyl branches. The synthesis was modified according to the procedure for our precisely placed methyl monomers (Figure 3).[14] Compound **11** is synthesized using sodium hydride with 11-bromo-1-undecene, followed by decarboxylation of the resulting diacid. The monoacid is reduced into the primary alcohol and directly converted to the bromide (**13**) using CBr_4. A single carbon homologation was performed by the addition of solid CO_2 to the Grignard of compound **13**. Once again its reduction was followed by the formation of the bromide **15**. Monomer **2** was obtained by quenching the Grignard of **15** with water. Noteworthy, the formation of the Grignard must be achieved using sonication, for production of the Grignard thermally causes compound **15** to dimerize. Again, the key difference between either methods (Figures 2 and 3) is the formation and reduction of the primary bromide (**15**) in Figure 3 using Mg/H_2O or if preferred the reduction of the tosylated alcohol with Super Hydride. The displacement of a primary tosylate using boron can produce the desired hydrocarbon monomer with minimal amounts of the eliminated compound (<5%).

The synthesis of symmetrical ethyl-branched dienes can be accomplished using methodologies outlined in either Figure 2 or 3. However, in an attempt to simplify our monomer synthetic procedure, we sought easier and more efficient ways to afford any length branch through simple organic transformations. Our initial endeavor focused on using Wittig couplings to produce monomers containing a "masked" branch yielding the correct ethyl branch upon exhaustive hydrogenation. In fact, the model PEs derived from monomers made through Wittig coupling

(17) Krishnamurthy, S.; Brown, H. C. *J. Org. Chem.* **1976**, *41*, 3064.

Table 1. Molecular Weights for ADMET Model EB Materials

		unsaturd copolymers (rel)[b]		saturd copolymers					
				rel (PS)[b]		universal[c]		LALLS[d]	
model EB copolymer	*n* (ethyl on every *n*th backbone carbon[a])	$M_w \times 10^{-3}$	PDI[e]	$M_w \times 10^{-3}$	PDI[e]	$M_w \times 10^{-3}$	PDI[e]	$M_w \times 10^{-3}$	PDI[e]
HPEB9	9	56.5	1.8	58.6	1.8	37.8	1.8	29.2	1.7
HPEB15W	15	53.1	1.9	54.2	1.9	31.2	1.9	23.8	1.8
HPEB21	21	56.1	2.0	54.1	1.8	36.5	1.9	28.6	1.7
HPEB21W	21	50.2	1.9	50.7	1.9	27.3	1.8	25.4	1.8

[a] Branch content based on the hydrogenated repeat unit. [b] Molecular weight data taken in tetrahydrofuran (40 °C) relative to polystyrene standards. [c] Molecular weight data taken in tetrahydrofuran (40 °C) using viscosity law calibration relative to polystyrene standards. [d] Molecular weight data taken using low-angle laser light scattering (LALLS) in tetrahydrofuran at 40 °C. [e] Polydispersity index (M_w/M_n).

(Figure 4) and ethyl acetoacetate addition (Figure 3) yield polymers having the exact primary structure. Their comparison will be discussed further.

Wittig monomers (Figure 4) were synthesized using an in-situ formation of the phosphorus ylide followed by direct attack on the corresponding ketone. The starting ketones were synthesized according to literature procedures.[18] The branch identity can be controlled by the starting bromoalkane used in the ylide precursor; for example, ethyl branches would be obtained from bromoethane. Their synthesis is done by refluxing the necessary bromoalkane with triphenylphosphine in diethyl ether, where the resulting salt is filtered, washed with excess ether, and dried prior to use. Upon addition of base to the salt/ketone slurry the solution turns yellow indicative of ylide formation. The reaction is complete within 30 min of base addition, and the product can be purified by flash chromatography in hexane. The clean chemistry and easy synthesis afforded by Wittig chemistry will allow formation of any branch length monomers readily from available, inexpensive starting bromoalkanes.

(B) ADMET Polymerization and Hydrogenation Chemistry. The proper choice of the appropriate catalyst system throughout this model study was crucial due to the differing monomer structures employed; only Grubbs' first generation[19] or Shrock's[20] catalyst could be used for pure α,ω-diene polymerizations. The Wittig monomers were polymerized only with Grubbs' catalyst, due to the presence of the "masked" branch, the trisubsituted olefin. Since we are modeling polymers containing exact primary structures, we have avoided all other ruthenium-based catalyst systems due to their propensity to isomerize external and internal olefins.[21]

Monomer **1** was exposed to Schrock's catalyst[20] under mild ADMET step polymerization conditions using typical catalyst loadings (1000:1, monomer:catalyst). All other monomers were polymerized using Grubbs' first generation catalyst. The chemistry proceeds cleanly to yield a linear, unsaturated polymer that is comprised of only one type of repeat unit, plus the usual amount of cyclics (<1−2%) found in bulk polycondensation conversions. Exhaustive hydrogenation of the unsaturated prepolymer was accomplished using either palladium on carbon (10 wt % Pd/C) or $RuHCl(CO)(PCy_3)_2$ (5 wt %); the homogeneous Ru catalyst was used with the trisubstituted olefinic prepolymers due to its literature applications in this area.[22] In both cases the hydrogenations were carried out over 5 days using 500 psi for Pd; however, higher pressure was needed (2000 psi) for the homogeneous catalyst to ensure complete hydrogenation. The polymers were purified by filtration and simple precipitation of the hydrogenation solution in acidic methanol (1 M). No side reaction was detectable by thin-layer chromatography (TLC) or nuclear magnetic resonance (NMR), and hydrogenation was verified by both infrared (IR) spectroscopy and NMR analysis. As previously observed, hydrogenation effectiveness is best monitored by IR. The 967−969 cm^{-1} absorption in the unsaturated polymer, which corresponds to the out-of-plane C−H bend in the alkene, completely disappears after successful hydrogenation. *This is the first example of any model EB copolymer being prepared containing precisely placed ethyl branches on each and every 9th, 15th, and 21st carbon along polyethylene's linear backbone*.

In the following sections, all polymers are named using the prefix **HP** (hydrogenated polymer) followed by the comonomer type (**EB**, ethylene/butane, or **EP**, ethylene/propylene), and the precise branch frequency (**21**); for example **HPEB21** is designated as hydrogenated ethylene/butene copolymer containing an ethyl branch on every 21st carbon. Due to the exact nature of the polymers produced, the comonomer content can be easily calculated using the branch frequency (*n*) following the relationship

$$\text{mol \% comonomer} = \frac{2}{n} \times 100$$

Table 1 confirms that the hydrogenation process does not alter the molecular weight of the unsaturated polymers in this study, which is consistent with our earlier experiments.[13−15] The saturated EB copolymers were analyzed by three molecular weight determination methods consisting of the use of an internal differential refractive index detector (DRI), differential viscosity

(18) Hopkins, T. E.; Wagener, K. B. *Macromolecules* **2003**, *36*, 2206.
(19) (a) Nguyen, S. T.; Grubbs, R. H.; Ziller, J. W. *J. Am. Chem. Soc.* **1993**, *115*, 9858. (b) Schwab, P.; France, M. B.; Ziller, J. W.; Grubbs R. H. *Angew. Chem., Int. Ed. Engl.* **1995**, *34*, 2039. (c) Schwab, P.; Grubbs, R. H.; Ziller, J. W. *J. Am. Chem. Soc.* **1996**, *118*, 100. (d) Grubbs, R. H.; Marsella, M. J.; Maynard, H. D. *Angew. Chem., Int. Ed. Engl.* **1997**, *36*, 1101. (e) Dias, E. L.; Nguyen, S. T.; Grubbs, R. H. *J. Am. Chem. Soc.* **1997**, *119*, 3887. (f) Dias, E. L.; Grubbs, R. H. *Organometallics* **1998**, *17*, 2758. (g) Trnka, T. M.; Grubbs, R. H. *Acc. Chem. Res.* **2001**, *34*, 18, and references therein.
(20) (a) Schrock, R. R.; Murdzek, J. S.; Bazan, G. C.; Robbins, J.; DiMare, M.; O'Regan, M. *J. Am. Chem. Soc.* **1990**, *112*, 3875. (b) Bazan, G. C.; Khosravi, E.; Schrock, R. R.; Feast, W. J.; Gibson, V. C.; O'Regan, M. B.; Thomas, J. K.; Davis, W. M. *J. Am. Chem. Soc.* **1990**, *112*, 8378. (c) Bazan, G. C.; Oskam, J. H.; Cho, H. N.; Park, L. Y.; Schrock, R. R. *J. Am. Chem. Soc.* **1991**, *113*, 6899. (d) Fox, H. H.; Schrock, R. R. *Organometallics* **1992**, *11*, 2763. (e) Feldman, J.; Murdzek, J. S.; Davis, W. M.; Schrock, R. R. *Organometallics* **1989**, *8*, 2260. (f) Oskam, J. H.; Schrock, R. R. *J. Am. Chem. Soc.* **1992**, *114*, 7588.
(21) (a) Lehman, S. E.; Wagener, K. B. *Inorg. Chim. Acta* **2003**, *345*, 190. (b) Sworen, J. C.; Pawlow, J. H.; Case, W.; Lever, J.; Wagener, K. B. *J. Mol. Catal. A: Chem.* **2003**, *194*, 69. (c) Bourgeois, D.; Pancrazi, A.; Nolan, S. P.; Prunet, J. *J. Organomet. Chem.* **2002**, *643*, 247. (d) Arisawa, M.; Terada, Y.; Nakagawa, M.; Nishida, A. *Angew. Chem., Int. Ed.* **2002**, *41*, 4732.
(22) (a) Martin, P.; McManus, N. T.; Rempel, G. L. *J. Mol. Catal. A: Chem.* **1997**, *126*, 115. (b) Otsuki, T.; Goto, K.; Komiya, Z. *J. Polym. Sci., Part A: Polym. Chem.* **2000**, *38*, 4661. (c) McManus, N. T.; Rempel, G. L. *J. Macromol. Sci., Rev. Macromol. Chem. Phys.* **1995**, *C35*, 239.

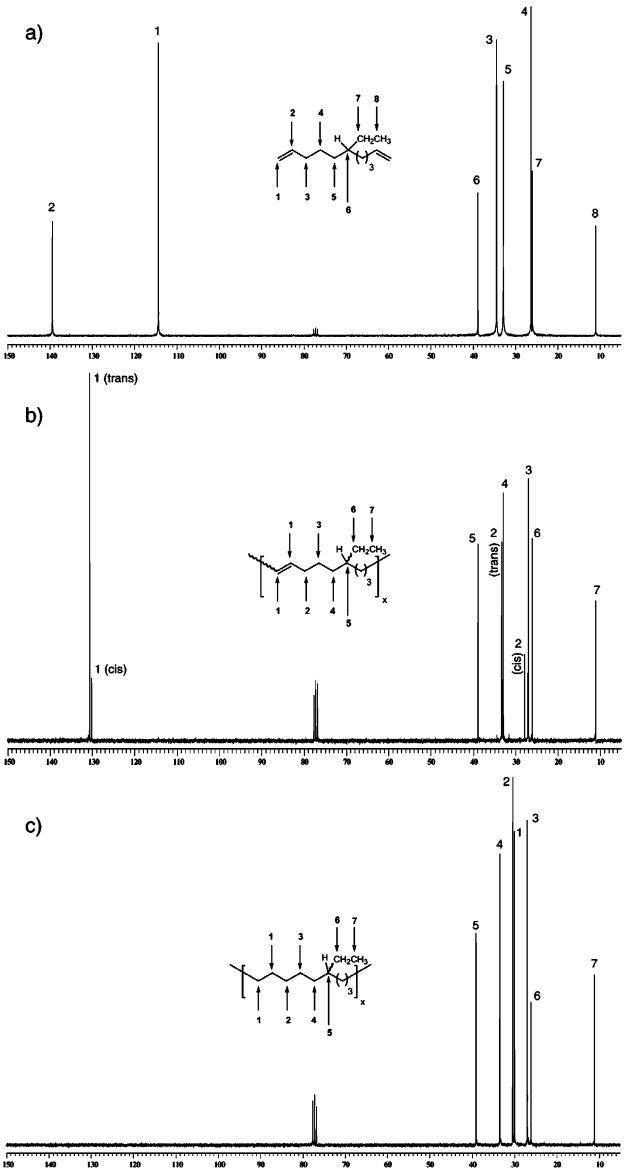

Figure 5. ^{13}C NMR of (a) monomer **1**, (b) **UPEB9**, and (c) **HPEB9**.

detector (DP), and a precision light scattering detector (LS). Using these three detectors in series, the molecular weights were determined by universal calibration (a plot of log intrinsic viscosity [η] $\times$ molecular weight vs retention time) calibrated using polystyrene (PS) and low-angle laser light scattering (LALLS). The results are shown in Table 1. The universal calibration data were generated by calibrating the retention times using 10 Polymer Laboratory polystyrene standards. As previously discussed for EP copolymer models,[14] these ADMET model EB copolymers exhibit molecular weights and polydispersities within a sufficient range to make it an excellent model for commercial grades of LLDPE produced via metallocene catalysis.[4−6]

(C) Structure Determination Using NMR and IR. Our goal in modeling PE-based materials is to develop an understanding of the relationship between the exact effect branch content and identity and a given model copolymer's micro- and macromolecular properties. A direct transfer of monomer branch content to the polymer is achieved using step metathesis chemistry

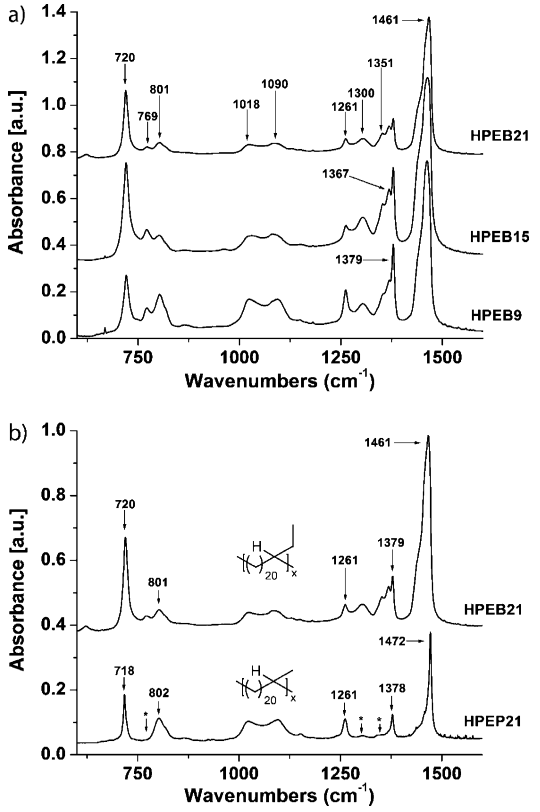

Figure 6. (a) Infrared spectra for ADMET EB copolymers and (b) IR comparison of precise methyl- and ethyl-branched copolymers (on every 21st carbon).

(ADMET). As a starting point we have used semiquantitative ^{13}C NMR as the primary tool for investigation to verify primary structure.

Figure 5 displays the ^{13}C NMR spectra for the conversion of monomer **1** to unsaturated polymer, **UPEB9** (Figure 5b); the ^{13}C spectrum for the fully saturated ADMET model EB copolymer possessing an ethyl branch on every 9th carbon, **HPEB9** is presented in Figure 5c. These NMR data confirm that the ADMET reaction has taken place. The absence of visible end groups (114.5 and 139.2 ppm) implies that high polymer has been obtained, a result consistent with the GPC results given earlier. Further, the internal olefin resonance at 130.62 ppm (Figure 5b) completely vanishes upon exhaustive hydrogenation of the double bonds (confirmed by IR, Figure 6).

The clean and complete nature of the transformations depicted in the spectra is typical for all ADMET model LLDPEs synthesized thus far,[14] data which illustrate the level of structural control that is possible when choosing step condensation chemistry as the method to model ethylene-*co*-α-olefin systems. Moreover, the ^{13}C NMR spectra of these ADMET copolymers reveal the exact chemical shifts of a particular branch point and its subsequent carbons. In effect, acyclic diene metathesis allows for a direct correlation between branch identity and observed NMR shift (ppm) due to the exact primary structure of the polymers. In the case of precise ethyl-branched copolymers, the observed shifts are 33.45 (α), 26.99 (β), 30.43 (γ), 30.31 (δ), 39.09 (methine), 26.12 (α′), and 11.12 ($1B_n$) ppm, which is in very good agreement with experimental[23,24] and predicted values.[25,26] These data suggest that ADMET model LLDPEs, in conjunction with high-field NMR experiments, could be used to derive new and improved mathematical parameters in the

structural study of branched polyethylene. A wealth of information can be collected concerning the amount, nature, and partitioning of branched PE materials using ^{13}C NMR studies.[27] The precisely branched ADMET PEs synthesized thus far offer a tremendous potential to study/model the direct impact a short-chain branch and its distribution have on the final structure−property relationships in ethylene-based materials. Nowhere is this more evident than in the NMR results presented here.

As previously observed in our model EP model copolymers, the utility of IR to observe and understand changes in structure is invaluable. In the past, Tashiro et al.[28] carried out a detailed study on the IR response of differing polyethylene crystal structures. In Figure 6, the saturated ADMET EB copolymer models clearly exhibit the characteristic shapes and absorption values (two single peaks at 1461 and 720 cm^{-1}), which suggests an unorganized packing structure. The limited correlation between IR and X-ray data in EB copolymers means that the exact structure cannot be determined from the absorbance spectra alone. However, following the vibrational analysis made for *n*-alkenes and disordered polyethylene we can make certain observations using the 1366, 1305, and 1352 cm^{-1} bands.[29]

Previously, the bands observed at 1366 and 1305 cm^{-1} were assigned to a kink and the 1352 cm^{-1} to a double gauche defect in PE materials.[28] The overall concentration of gauche and kink methylene sequences for our ADMET EB copolymers is reduced with the decrease in branch defect content. This trend can be observed by the comparison of these defect bands versus the $-CH_2-$ scissoring at 1461 cm^{-1}. Also, the ratio of these defect bands (1366, 1305, and 1352 cm^{-1}) relative to the methylene wagging vibration at 1261 cm^{-1} shows a unique pattern. Close inspection reveals that the ratio of all three disordered vibrations are equal relative to each other; however, their ratio to 1461 cm^{-1} changes depending on the branch content and crystallinity. Of course, both **HPEB9** and **HPEB15** are amorphous at the recorded spectra temperature, while **HPEB21** is semicrystalline. The observed disordered ratio trend can also be observed using the 801 and 769 cm^{-1} vibrations (visible with EB copolymers[30]). The peaks most likely originate from a methylene rock and proceed with a similar up/down ratio when the defect content and crystallinity change. While at present the exact cause of these vibrations and variable intensities cannot be correlated to structural information in our EB copolymers, we can compare them to our precise methyl-branched copolymers as well as theoretical models (Figure 6b).

The higher content of these defects is in accord with the higher steric demand of the ethyl branch over the methyl branch. Further, the majority of the methyl branches are known to incorporate into the repeating methylene sequences.[31] Of course, under equilibrium conditions the branches, even methyl, are assumed to be rejected from the crystallites.[32] Equilibrium is seldom reached during crystallization, however, thereby favoring an intermediate situation where the partial segregation of branches exists between the amorphous and crystal regions.[33] This equilibrium, for branches longer than methyl, can be shifted by the crystallization conditions to favor inclusion or exclusion.[31a,34] On this basis, the bulk of the ethyl side group is at the boundary between total exclusion and inclusion within the crystal lattice.

The intermediate situation of phase partitioning chain defects seems most likely, and there have been numerous experimental,[27,31b,35] theoretical,[36−39] and molecular modeling studies[40] to help define a mechanism for branch inclusion. Typically, X-ray diffraction coupled with high-field ^{13}C NMR has been used to determine branch inclusion. For ethyl-branched polymers, the proportion of ethyl branch inclusion was determined to be a function of SCB concentration and was estimated at 10:1 (17 SCB/1000C) and 5:1 (21 SCB/1000C) between the amorphous and crystalline regions.[27a,31b,34] More recently, studies have assumed the existence of branch incorporation by considering possible structural perturbations and conformational defects. These studies have proposed interstitial sites along the polymer chains, known as kinks,[36,37] arising from conformational gauche defects (2g1 defects) being the most common.[38] These 2g1 defects have been proposed to be large enough for ethyl branches.[36a,39] In fact, the gtg (2g1) conformation can be observed using IR and assigned the 1366 and 1305 cm^{-1} absorptions.

As mentioned earlier, our EB copolymers exhibit high concentrations of the kink (tttgtgttt) defect. The concentration of these defects relative to the double gauche (1351 cm^{-1}) remains constant throughout the branch content. Also, it would seem that the distorted trans segments (shoulder of the 1461 cm^{-1} absorption) hold this constant relationship as well. The

(23) (a) Liu, W.; Ray, D. G., III; Rinaldi, P. L. *Macromolecules* **1999**, *32*, 3817. (b) Axelson, D. E.; Levy, G. C.; Mandelkern, L. *Macromolecules* **1979**, *12*, 41. (c) Kuroda, N.; Nishikitani, Y.; Matsuura, K.; Ikegami, N. *Macromolecules* **1992**, *25*, 2820. (d) Lee, D. H.; JHo, J. Y. *Polym. Bull.* **1997**, *38*, 665.

(24) Rossi, A.; Zhang, J.; Odian, G. *Macromolecules* **1996**, *29*, 2331.

(25) Glowinkowski, S.; Makrocka-Rydzyk, M.; Wanke, S.; Jurga, S. *Eur. Polym. J.* **2002**, *38*, 961.

(26) (a) Grant, D. M.; Paul, E. G. *J. Am. Chem. Soc.* **1964**, *86*, 2984. (b) Lindeman, L. P.; Adams, J. Q. *Anal. Chem.* **1971**, *43*, 1245.

(27) (a) Pérez, E.; VanderHart, D. L.; Crist, B., Jr.; Howard, P. R. *Macromolecules* **1987**, *20*, 78. (b) VanderHart, D. L.; Pérez, E. *Macromolecules* **1986**, *19*, 1902.

(28) Tashiro, K.; Sasaki, S.; Kobayashi, M. *Macromolecules* **1996**, *29*, 7460.

(29) (a) Synder, R. G.; Maroncelli, M.; Qi, S. P.; Strauss, H. L. *Science* **1981**, *214*, 188. (b) Maroncelli, M.; Qi, S. P.; Strauss, H. L.; Synder, R. G. *J. Am. Chem. Soc.* **1982**, *104*, 6327. (c) Kim, Y.; Strauss, H. L.; Synder, R. G. *J. Phys. Chem.* **1989**, *93*, 7520.

(30) (a) Yang, Y.-C.; Geil, P. H. *Makromol. Chem.* **1985**, *186*, 1961. (b) Wool, R. P. *Polym. Eng. Sci.* **1980**, *20*, 805.

(31) (a) Baker, C. H.; Mandelkern, L. *Polymer* **1966**, *7*, 71. (b) Pérez, E.; Vanderhart, D. L. *J. Polym. Sci., Part B: Polym. Phys.* **1987**, *25*, 1637. (c) Richardson, M. J.; Flory, P. J.; Jackson, J. B. *Polymer* **1963**, *4*, 221.

(32) (a) Flory, P. J. *J. Chem. Phys.* **1949**, *17*, 223. (b) Flory, P. J. *Trans. Faraday Soc.* **1955**, *51*, 848.

(33) Eichorn, R. M. *J. Polym. Sci.* **1958**, *31*, 197.

(34) Perez, E.; Bello, A.; Perna, J. M.; Benavente, R.; Martinez, M. C.; Aguilar, C. *Polymer* **1989**, *30*, 1508.

(35) (a) Cutler, D. J.; Hendra, P. J.; Cudby, M. E. A.; Willis, H. A. *Polymer* **1977**, *18*, 1005. (b) Vile, J.; Hendra, P. J.; Willis, H. A.; Cudby, M. E. A.; Bunn, A. *Polymer* **1984**, *25*, 1173. (c) France, C.; Hendra, P. J.; Maddams, W. F.; Willis, H. A. *Polymer* **1987**, *28*, 710. (d) McFaddin, D. C.; Russell, K. E.; Kelusky, E. C. *Polym. Commun.* **1988**, *29*, 258. (e) Hosoda, S.; Nomura, H.; Gotoh, Y.; Kihara, H. *Polymer* **1990**, *31*, 1999. (f) Hay, J. N.; Zhou, X.-Q. *Polymer* **1993**, *34*, 1002. (g) Russell, K. E.; McFaddin, D. C.; Hunter, B. K.; Heyding, R. D. *J. Polym. Sci., Part B: Polym. Phys.* **1996**, *34*, 2447. (h) Hosoda, S.; Hori, H.; Yada, K.; Nakahara, S.; Tsuji, M. *Polymer* **2002**, *43*, 7451.

(36) (a) Pechhold, W. *Kolloid Z. Z. Polym.* **1968**, *228*, 1. (b) Baltá-Calleja, F.-J.; Gonzalez Ortega, J. C.; Martinez de Salazar, J. *Polymer* **1978**, *19*, 1094. (c) Heink, M.; Häberle, K.-D.; Wilke, W. *Colloid. Polym. Sci.* **1991**, *269*, 675. (d) Seguela, R.; Rietsch, F. *J. Polym. Sci., Polym. Lett. Ed.* **1986**, *24*, 29.

(37) (a) Vonk, C. G. *J. Polym. Sci.* **1972**, *38*, 429. (b) Kortleve, G.; Tuijnman, C. A. F.; Vonk, C. G. *J. Polym. Sci., Polym. Phys. Ed.* **1972**, *10*, 123. (c) Vonk, C. G.; Pijpers, A. P. *J. Polym. Sci., Polym. Phys. Ed.* **1985**, *23*, 2517.

(38) Wunderlich, B. Crystal Structure, Morphology, and Defects. *Macromolecular Physics*; Academic Press Inc.: New York, 1973; Vol. 1.

(39) (a) Gaucher, V.; Séguéla, R. *Polymer* **1994**, *35*, 2049. (b) Martinez de Salazar, J.; Baltá-Calleja, F.-J. *J. Cryst. Growth* **1980**, *48*, 283. (c) Scherr, H.; Pechhold, W.; Blasenbrey, S. *Kollid Z. Z. Polym.* **1970**, *238*, 396. (d) Baltá-Calleja, F -J.; Hosemann R. *J. Polym. Sci., Polym. Phys. Ed.* **1980**, *18*, 1159.

(40) (a) Baker, A. M. E.; Windle, A. H. *Polymer* **2001**, *42*, 681. (b) Napolitano, R.; Pucciariello, R.; Villani, V. *Macromol. Theory Simul.* **1994**, *3*, 623.

nearly constant ratio of these bands versus defect content for our EB copolymers suggests that defect equilibrium is independent of methylene sequence length. The thermal analysis of these polymers, discussed later, shows that **HPEB9** is amorphous most likely because of the short sequences of trans methylenes between branch kinks. As the branch frequency decreases, the resulting longer run length of trans segments enables the polymer to crystallize, depending on the temperature as seen for **HPEB21**.

The larger steric demand has brought about a large increase in the gauche and kick defects relative to ADMET EP copolymers (Figure 6b) as well as a new observed vibration (wag) at 769 cm^{-1}. These defects are small and only slightly observed for the methyl-branched **HPEP21**. There is also a shift in the methylene scissoring vibration from 1472 cm^{-1} for **HPEP21** to 1461 cm^{-1} for **HPEB21**. Although the band positions are slightly different from a typical orthorhombic crystal of PE,[28] observed at 1472 and 1463 cm^{-1}, our EP and EB copolymers encompass both peaks, respectively. To further delineate the copolymers structure, the thermal behavior of these materials was explored.

(D) Thermal Analysis. Numerous thermal behavior studies have been performed on commercially produced LLDPEs[41] and EB copolymers containing a statistical distribution of ethyl branches.[4c,5,6a,b,8a,b,27a,42−48] Similar to the results obtained for EP copolymers, studies on randomly branched EB copolymer systems have shown that the density, enthalpy, degree of crystallinity, and peak melting/crystallization points all decrease as the amount of defect content (ethyl branches) is increased.

Like EP copolymers, the melting behavior of EB systems is influenced by the amount of SCB; however, the SCB distribution (SCBD) is by far the most determinant factor on the final physical properties of a given material. The major problem arising during modeling studies on ethylene-based polymers is the compositional heterogeneity normally encountered for these statistically branched materials. In this way, ADMET EB copolymers present the advantage of being well-defined materials with a homogeneous distribution of defects along the backbone. Thus they make excellent substances with which to model the effect that SCB and SCBD have on the final materials response of ethylene-based materials.

Figure 7 shows a calorimetric comparison between the saturated ethyl (**HPEB9**) versus fully saturated methyl-branched polymer (**HPEP9**). Both materials possess precise branch

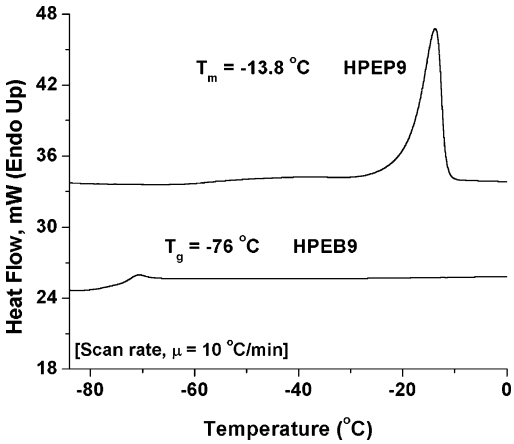

Figure 7. DSC comparison of (1, top) **HPEP9** (ADMET model ethylene/propylene copolymer with a methyl on each 9th carbon) and (2, bottom) **HPEB9** (ADMET model ethylene/butylene copolymer with an ethyl on each 9th carbon.

distribution along the hydrocarbon backbone. Previously studied model EB copolymers, made from hydrogenated poly(butadienes), have exhibited ill-defined melts for branch contents as high as 106 ethyls/1000 carbons.[44] In contrast, the ADMET model EB copolymer **HPEB9**, possessing 111 ethyls/1000 carbons, shows no detectable melting point in the range studied here, suggesting a completely amorphous behavior. This result is interesting when compared to the narrow melting point exhibited by the ADMET model EP copolymer (**HPEP9**) with the same branch content (Figure 7).

The only viable explanation for this difference is that methyl branches are readily incorporated into the crystal lattice, whereas the steric demands of the ethyl branch preclude its taking part in the crystallization process at this level of precise branch distribution. In an effort to produce EB copolymers containing crystalline segments the average methylene run length (MSL) was increased to produce both model polymers **HPEB15** and **HPEB21**. Our modeling polymerization chemistry, ADMET, lends itself perfectly for this task.

As shown previously we are able to modify the backbone of our model polymers by simple monomer manipulation. Figures 2 and 3 illustrate that we have developed a routine synthesis to create monomers containing an ethyl branch and any level of branch content ('*R*'/1000 carbons). In fact, the model copolymers containing an ethyl branch on every 21st backbone carbon were synthesized with two different methodologies. Utilizing the Wittig reaction along with the appropriate ruthenium polymerization catalyst, we were able to make the total synthesis viable for modeling PE on a large scale. Overall this new synthetic approach allows for modeling material properties and perhaps polymer blends on industrial scales. Of course, for the Wittig methodology to be a viable method for monomer synthesis, the trisubstituted olefin must remain inactive throughout the polymerization. If at any time the trisubstituted olefin engages in metathesis, even after all terminal olefins have reacted, the polymer primary structure would be altered. To determine if the pendent olefin in the Wittig monomers were actually inactive in the ADMET polymerization cycle, both monomers **2** and **3** were synthesized and compared (Figure 8).

To prove the Wittig method of producing monomers was adequate for modeling EB-branched polyolefins, **HPEB21** was synthesized from a purely α,ω diene monomer obtained by the

(41) (a) Wilfong, D. L.; Knight, G. W. *J. Polym. Sci., Part B: Polym. Phys.* **1990**, *28*, 861. (b) Starck, P. *Polym. Int.* **1996**, *40*, 111. (c) McKenna, T. *Eur. Polym. J.* **1998**, *34*, 1255. (d) Mirabella, F. M. *J. Polym. Sci., Part B: Polym. Phys.* **2001**, *39*, 2800. (e) Burfield, D. R.; Kashiwa, N. *Makromol. Chem.* **1985**, *186*, 2657.
(42) Kim, M.-H.; Phillips, P. J. *J. Appl. Polym. Sci.* **1998**, *70*, 1893.
(43) Crist, B.; Howard, P. R. *Macromolecules* **1999**, *32*, 3057.
(44) Crist, B.; Williams, D. N. *J. Macromol. Sci. Phys.* **2000**, *B39*, 1.
(45) Zhang, M.; Lynch, D. T.; Wanke, S. E. *Polymer* **2001**, *42*, 3067.
(46) (a) Crist, B.; Claudio, E. S. *Macromolecules* **1999**, *32*, 8945. (b) Xu, J. T.; Xu, X. R.; Chen, L. S.; Feng, L. X. *J. Mater. Sci. Lett.* **2000**, *19*, 1541. (c) Xu, X.; Xu, J.; Feng, L.; Chen, W. *J. Appl. Polym. Sci.* **2000**, *77*, 1709. (d) Xu, J.; Xu, X.; Feng, L. *Eur. Polym. J.* **1999**, *36*, 685. (e) Van Ekeren, P. J.; Ionescu, L. D.; Mathot, V. B. F.; Van Miltenburg, J. C. *Thermochim. Acta* **2002**, *391*, 185. (f) Starck, P.; Rajanen, K.; Löfgren, B. *Thermochim. Acta* **2003**, *395*, 169. (g) Jokela, K.; Väänänen, A.; Torkkeli, M.; Starck, P.; Serimaa, R.; Löfgren, B.; Seppälä, J. *J. Polym. Sci., Part B: Polym. Phys.* **2001**, *39*, 1860.
(47) Adisson, E.; Ribeiro, M.; Deffieux, A.; Fontanille, M. *Polymer* **1992**, *33*, 4337.
(48) (a) Alamo, R. G.; Mandelkern, L. *Macromolecules* **1989**, *22*, 1273. (b) Alamo, R. G.; Viers, B. D.; Mandelkern, L. *Macromolecules* **1993**, *26*, 5740.

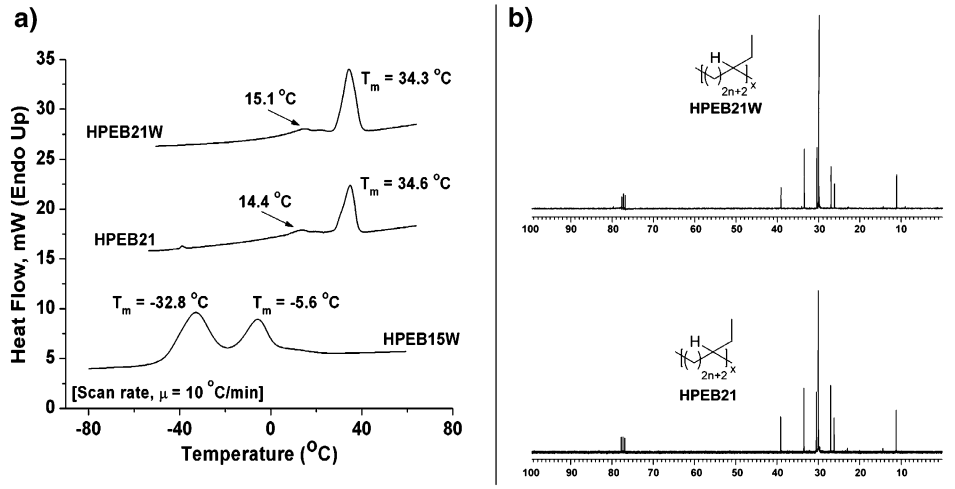

Figure 8. (a) DSC comparison for **HPEB21**, **HPEB15W**, and **HPEB21W**. (b) ^{13}C NMR of **HPEB21** and **HPEB21W**.

procedure outlined in Figure 3. The polymer was then used as the reference and compared to the Wittig produced copolymer (**HPEB21W**). The easiest and most effective method to make a structure comparison between **HPEB21** and **HPEB21W** was close inspection of both ^{13}C NMR and differential scanning calorimetry (DSC). This comparison would lead to an identical response to the external stimuli if both polymer's macromolecular behavior were the same. Further, the thermograph and carbon spectra of both polymers would be equal if the primary structures were equal. In fact, if at anytime throughout the metathesis cycle the trisubstituted olefin in **UPEB21W** becomes metathesis active, one or both of these techniques would detect the structural change. Figure 8 reveals that both polymers have an identical carbon spectrum and exhibit the same nearly monomodal melting profile containing two distinct peak melting temperatures. The enthalpy ratio between these two melting peaks is the same regardless of the polymer synthetic methodology.

The precise nature of the branch location or constant MSL produces a semicrystalline polymer favoring a single crystalline region (T_m = 34.3 °C). Comparison of model EB copolymers synthesized using either metallocene[42,45] or hydrogenated polybutadienes,[8b,44] at the same level of branch content, shows very ill-defined endotherms. However, when **HPEB21** (ethyl branch) is compared to the precise methyl-branched model **HPEP21**, studied previously, the latter has a higher peak melting temperature (62 °C) and a higher melting enthalpy (103 J/g). The EP model copolymer also exhibits a sharp melting profile with no premelting in contrast to the rather large premelting thermograph seen for **HPEB21**. To ascertain the semicrystallinity limit in our model EB copolymers, the methylene sequence length was reduced to produce **HPEB15W**. This model copolymer, containing an ethyl branch on every 15th carbon, was synthesized using the Wittig approach only.

The reduction of the methylene sequence length causes the melting point to drop below room temperature. The polymer still exhibits semicrystallinity, but increasing the defect content results in a bimodal melting profile. Similar results have been observed for continuously cooled hydrogenated polybutadienes at much higher branch content.[44] Apparently, precisely placed ethyl-branched EB copolymers have a single sharp melting profile for copolymers containing approximately 50−60 ethyl branches per 1000 total carbons. The crystal formation and/or the crystallization kinetics also change when the overall branch content is increased. For example, when going from the amorphous **HPEB9** to the semicrystalline **HPEB21,** the melting profile becomes bimodal. These two different melting crystals may originate from the same source when comparing **HPEB15** and **HPEB21,** but regardless of crystal origin the enthalpy ratio increases when going from **HPEB15** to **HPEB21,** favoring the higher melting crystal. We have used annealing experiments on **HPEB21W** in an effort to force the copolymer to prefer a single crystal form. The same experiments could have been conducted with **HPEB15W**; however, we focused on **HPEB21W** primarily because of its higher melting temperature (above room temperature).

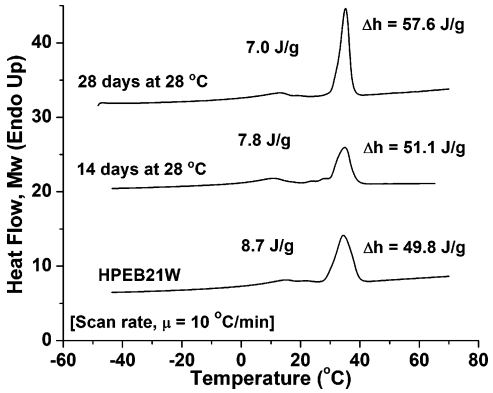

Figure 9. DSC thermograph of (1, bottom) **HPEB21W**, (2, middle) annealed **HPEB21W** for 14 days at 28 °C, and (3, top) annealed **HPEB21W** for 28 days at 28 °C.

Figure 9 illustrates that the EB copolymer **HPEB21W** can be manipulated by annealing the sample. The sample was initially annealed in the DSC at the leading edge of the higher melting crystal; in the case of **HPEB21** the ideal temperature was found at 28 °C. Upon annealing the sample for 14 days (Figure 9), the reduction of the lower melting crystal was substantial and produced a polymer with a precise narrow peak melting temperature of 34.4 °C. In an effort to reduce the premelting in **HPEB21W,** the annealing experiment was carried outside in an isothermal bath at 28 °C for 28 days (Figure 9). Figure 9 illustrates that the polymer's small endotherms and premelting observed after 14 days have been eliminated,

producing a distinct, narrow single melting peak for **HPEB21-(W)**. The melting profile for our copolymer containing an ethyl branch precisely placed on every 21st carbon exhibits the same behavior as our model EP copolymers, albeit at lower temperatures.

In this light, consensus has it that melting temperatures, crystallinity, and lamella thickness are a function of branch content and are relatively independent of branch size (excluding methyl). Since the identity of the branch (again, excluding methyl) has little effect on the crystal nature of LLDPE due to branch exclusion, the comonomer incorporation is the most important factor influencing the polymer's behavior. These issues are a direct result of catalyst choice and polymerization conditions; for example, a metallocene EB copolymer (homogeneous) has a lower T_m (26 °C) than a polymer with the same average branch content (30 SCB/1000C) but synthesized with a heterogeneous catalyst system.[45] These melting differences have been suggested to originate from the thick unbranched crystal formation witnessed in all heterogeneous systems. The more homogeneous branched system lacks the longer unbranched sequences and as a result thinner crystals and lower melting temperatures. Our ADMET-produced polymers have perfect and constant MSL through every repeating sequence so a comparison between homogeneous, heterogeneous, and our copolymers is important.

Correlations between branch content and melting temperature in EB copolymers have been investigated for metallocene, Ziegler−Natta (Z−N), and hydrogenated polybutadienes (HPB).[44,45,47,48] From the data reported, the peak melting temperature decreases with more controlled polymerization conditions. For the same branch content T_m follows the trend 95, 88, and 62 °C for HPB, Z−N, and metallocene, respectively. Of course, ADMET copolymers have more control of the polymer's primary structure, even more than those observed for any metallocene catalyst. Having theoretically no heterogeneity in branch incorporation (or MSL), ADMET copolymers should exhibit lower melting points than metallocene copolymers, most likely resulting from smaller crystallite formation. Relating the branch content of our ADMET copolymers to the derived chain-addition models agrees with this assumption. Indeed, if **HPEB21** was produced by chain addition, the level of branch content (43.5 SCB/1000 carbons) would predict a melting point of ∼60 °C (actual T_m = 34.5 °C).[45] Furthermore, the enthalpy of fusion of our ADMET EB copolymers is much higher (∼57 J/g) than either metallocene (∼30 J/g) or Z−N (∼42 J/g) copolymers. These results are consistent with ADMET producing more homogeneous sequence lengths relative to any chain-addition polymerization. Further studies are being conducted to investigate the packing of these unique materials and delineate correlations to previously synthesized EP model copolymers.[49]

Conclusions

Acyclic diene metathesis polymerization has proven to control the primary structure of ethylene/1-butene copolymers resulting in linear polyethylene containing only ethyl branches. In this effort, a simple synthetic method has been developed to produce exact linear model polymers on an industrial scale using ketodienes. The inherent ability of metathesis to control the polymers branch identity and placement has profound effects on the thermal and crystal behavior of these distinct EB materials resulting in a new class of LLDPEs.

The structural investigation has shown that these ADMET EB copolymers favor ethyl branch inclusion, producing a similar crystal structure obtained for our EP model copolymers. Moreover, these copolymers exhibit distorted methylene sequences with high concentrations of kink, gauche, and double gauche defects. The inter- and intrahomogeneity of the sequence length distribution in these materials produces lower melting points and higher melting enthalpies when compared to chain-propagated EB polymers. In fact, the thermal behavior of these materials concludes that the MSL and its distribution are more controlled versus chain-addition chemistry and single-site metallocene systems. Step polymerization also produces narrow monomodal melting profiles when branch content reaches approximately 45 ethyl branches/(1000 carbons) or 9 mol % 1-butene.

We are currently continuing this branched polyethylene research by gathering a better base of scattering data and understanding the differences between random and precise branch content. In addition, we are investigating precisely branched linear, low-density materials containing hexyl and ultimately longer defects.

Acknowledgment. We wish to thank the National Science Foundation (Grant No. DMR9806492) for financial support of this research.

Supporting Information Available: Detailed characterization and experimental data for all synthesized monomers and polymers. This information is available free of charge via the Internet at http://pubs.acs.org.

JA047850P

(49) Lieser, G.; Wegner, G.; Smith, J. A.; Wagener, K. B. *Colloid Polym. Sci.* **2004**, *282*, 773.